AMPA 2 (GRIA2) (8, 9), potentially as downstream effectors of the target molecules of mood stabilizers.

Since these previous studies investigating the molecular mechanisms of mood stabilizers focused primarily on neuronal cells and used either neuronal cells or brain tissues, which are heterogeneous mixtures of various types of neuronal, glial, and vascular cells, the biological effects of mood stabilizers on astrocytes remain largely unknown. Since the function of astrocytes includes regulation of the extracellular concentrations of ion and neurotransmitters, modification of synaptic efficacy, maintenance of the blood-brain barrier, and structural as well as trophic support of neurons and oligodendrocytes (10–14), it is reasonable to expect that mood stabilizers may exert at least part of their mood-stabilizing and neuroprotective effects by affecting these astrocytic functions. Indeed, some studies suggest the potential involvement of astrocytes in the pathogenesis of BD. Many postmortem brain studies of patients with BD have demonstrated abnormalities in the density and shape of glial cells, as well as decreased levels of the astrocyte marker, glial fibrillary acidic protein (GFAP) (15). Glia are markedly reduced in the subgenual prefrontal cortex of patients with BD, and this reduction is most prominent in patients with familial BD (16). Mean glial density is significantly reduced in sublayers IIIc and Vb of the prefrontal cortex in patients with BD, whereas the mean size of glial cell bodies is increased in layers I and IIIc, which can be attributed to the increased density of extra-large glia in those layers (17). Although previous studies have also shown that the density and size of cortical neurons are reduced in mood disorders, these neuronal reductions are more subtle compared to the glial alterations (18). Furthermore, astrocyte-specific GFAP transcripts are significantly decreased in white matter, and tend to be decreased in gray matter of the anterior cingulate cortex of patients with BD (19). The decrease in GFAP expression was confirmed in a proteomic study of the frontal cortex of patients with BD (20). S100B, which is produced and secreted by astrocytes, is significantly increased in the serum of patients during episodes of manic and depressive states (21). S100B exerts trophic and/or toxic effects on neuronal and glial cells depending on its concentration and has been reported to be a susceptibility gene for a subgroup of BD patients presenting with psychotic symptoms (22). Thus, while current evidence is not conclusive, it does seem to suggest that a dysfunction or a loss of astrocytes may at least in part underlie the pathogenesis of BD.

Moreover, several studies have shown that mood stabilizers exert biological effects on astrocytes. Li has been shown to suppress the extracellular signal-regulated protein kinase pathway (23), whereas VPA increases the expression of neurotrophic factors in astrocytes (24). Li, VPA, and CBZ decrease *myo*-inositol uptake activity (25) and kainate receptor subunit GluR6 (GRIK2) expression in astrocytes (26), whereas Li, VPA, and CBZ increase the pH and cytosolic phospholipase A2 (cPLA2) levels in astrocytes (27, 28). It is worth noting that while these mood stabilizers have distinct chemical characteristics, they affect common molecular and cellular pathways in astrocytes.

Taken together, these studies suggest glial abnormalities in patients with BD and an effect of mood stabilizers on certain genes in astrocytes. However, the effects of mood stabilizers on astrocytes have been much less characterized compared to their effects on neuronal cells. To identify the most prominent biological effect of mood stabilizers on human astrocytes, we conducted microarray-based comprehensive gene expression analyses of a human astrocyte cell line treated with four major mood stabilizers, Li, VPA, CBZ, and LTG, and corresponding controls. We found a transcriptional regulation that was unique to each mood stabilizer and common molecules that were regulated by all four mood stabilizers. Fasciculation and elongation protein zeta 1 (FEZ1) was the only gene that was upregulated by all four mood stabilizers at both the mRNA and the protein expression levels. This finding points to FEZ1 as a candidate gene involved in the mechanism responsible for the mood-stabilizing effect of the tested drugs.

Materials and methods

Cell lines and cultures

The astrocyte-derived human cell line U-87 MG and the neuron-derived human cell line SK-N-SH were purchased from the American Type Culture Collection. The human oligodendroglioma cell line (OL) was a gift from Dr. Juan Carlos De La Torre from the Scripps Research Institute, La Jolla, CA, USA. Primary astrocytes from the human brain cortex (ACBRI 371) were purchased from Applied Cell Biology Research Institute, Kirkland, WA, USA. For the microarray studies, U-87 MG cells (6×10^8 cells) were suspended in 30 ml of Modified Eagle's Medium [(MEM) Sigma-Aldrich, St. Louis, MO, USA] containing 10% inactive fetal bovine serum (Biological Industries, Beit-Haemek, Israel) and divided into six plastic T75 cell culture flasks (Nalge Nunc Int., Rochester, NY, USA). Li (Kanto

Chemical, Tokyo, Japan) and VPA (Sigma-Aldrich) were dissolved directly in MEM at therapeutic concentrations of 0.75 mM and 0.5 mM, respectively. Cells cultured in non-treated (drug-free) MEM were used as controls to evaluate the effects of Li and VPA. The water-insoluble agents CBZ (Sigma-Aldrich) and LTG (Sigma-Aldrich) were dissolved in 100% dimethyl sulfoxide (DMSO) at 33.3 mM and 3.33 mM, respectively (666.6 times the final concentrations) and then resuspended into MEM at 50 μM and 5 μM, respectively, each of which is within the therapeutic range. Since the final DMSO concentration of CBZ- and LTG-containing MEM was 0.15%, control cells were cultured in MEM containing 0.15% DMSO. U-87 MG cells were evenly split into six flasks in MEM and maintained at 37°C in a humidified atmosphere containing 5% CO_2 for 18 hours. The media were replaced with MEM which included Li-, VPA-, CBZ-, LTG-, DMSO-containing, or non-treated MEM and cultured in the same chamber for five days. After a week of exposure to each condition, the media were removed from each flask, and the cells were washed and collected in phosphate buffered saline. To distinguish the biological effects of the mood stabilizers from artifacts, all of the experimental procedures were replicated following completion of the first set of experiments, and two sets of six types of cultured cells were subjected to the following microarray experiments. To validate the microarray expression data by quantitative real-time PCR (qRT-PCR), U-87 MG cells (1×10^8 cells) were cultured in the six different media in the presence or absence of mood stabilizers for five days, in the same manner as in the microarray experiment. For each conditioned medium, the cell culture was replicated in six independent T75 flasks (in total, 6 types of media × 6 replicates = 36 samples). To evaluate the effect of high-dose mood stabilizer treatments on protein levels by western blot, cells were cultured for five days with higher concentrations (near the maximum limit of the therapeutic ranges) of Li, VPA, CBZ, or LTG (1.2 mM, 1 mM, 100 μM, and 50 μM, respectively). Given the limited quantity of ACBRI371 cells, U-87 MG cells were used for microarray and qRT-PCR analyses, while ACBRI371 cells were used only to determine FEZ1 localization by immunocytochemistry.

RNA extraction and microarray experiments

Total RNA was extracted, DNase-digested, and purified using the RNeasy Mini Kit, RNase-free DNase I, and the RNeasy MinElute Cleanup Kit (Qiagen, Valencia, CA, USA). The RNA integrity number (RIN) for each RNA sample was confirmed to be > 9.8 using the Agilent 2100 Bioanalyzer (Agilent, Santa Clara, CA, USA), and the ribosomal RNA S28/S18 ratio was > 1.9. From the 12 total RNA samples, biotinylated cRNA were synthesized and applied to Illumina BeadChips according to the manufacturer's directions. In brief, biotinylated cRNA was prepared from 500 ng of total RNA using the Illumina Ambion RNA Amplification Kit (Ambion, Austin, TX, USA). The biotinylated cRNA samples were hybridized to Illumina Human-6v2 Expression BeadChips (Illumina, San Diego, CA, USA). Each BeadChip was washed and scanned with Illumina Bead Station 500X.

Data analysis and selection criteria for mood-stabilizer-regulated genes

The inter-array variation among 12 BeadChip microarrays (for 6 types of media × experimental duplication) was normalized using average normalization after subtracting the background signal intensities. The probability of observing a certain signal intensity level for a set of beads lacking specific probe-target hybridization was calculated as the detection p-value for each probe. The above procedure was performed using Illumina BeadStudio 3.1 software (Illumina). Among the 48,701 transcripts designed on the BeadChip, 11,214 transcripts with signal intensities > 20 and with detection p-values of < 0.05 in all of the 12 U-87 MG samples were considered reliably detectable, and the signal intensities of these transcripts in Li- and VPA-treated cells and in non-treated cells were compared. The signal intensities in CBZ- and LTG-treated cells and in DMSO-treated cells were also compared. Transcripts with consistent fold changes of > 1.2 or < 0.833 in both experimental duplicates were defined as *mood-stabilizer-induced* or *mood-stabilizer-suppressed* genes, respectively. Changes in mRNA expression are consistent among duplicated microarrays when altered genes are selected with a cut-off fold change of > 1.2 or < 0.833, criteria widely used in microarray analyses (29–31). The probability of observed number of overlapping genes in proportion to the expected number was calculated based on hypergeometric distribution, and a p-value of < 0.05 was considered statistically significant. Assuming that among the 48,701 probes, the number of genes altered by drugs A and B are 'a' and 'b' respectively, and effects of treatments are irrelevant, the expected number of overlapping genes between the lists of genes altered by drugs A and B is (a × b)/48,701.

Hierarchical clustering

To evaluate similarities between the effects of mood stabilizers on expression profiles, the fold change values for the signal intensities of mood-stabilizer-treated samples, relative to the signal intensities determined for the control samples (Li/non-treated control, VPA/non-treated control, CBZ/DMSO-treated control, LTG/DMSO-treated control), were log2 transformed and subjected to an average linkage hierarchical clustering analysis using Genesis software 1.7.5 (available at http://www.genome.tugraz.at). To minimize the confounding effect of DMSO added to CBZ, LTG, and the corresponding control samples, 1,306 genes differentially expressed between the non-treated and DMSO-treated control samples with a fold change of > 1.2 or < 0.833 in at least one of the duplicated experiments were eliminated from the analyses. Among the 11,214 reliably detectable transcripts (with signal intensities > 20 and with detection p-values < 0.05 in all 12 U-87 MG samples), 9,908 transcripts, levels of which were similar between DMSO-treated and untreated samples, were subjected to hierarchical clustering analysis.

Quantitative real-time PCR experiments

Total RNA was extracted from the 36 cell samples [6 types of media (Li, VPA, CBZ, LTG, DMSO-treated control, non-treated control) × 6 replicates] in the same manner employed for the microarray experiment and subjected to cDNA synthesis with random primers using the SuperScript VILO cDNA synthesis kit (Invitrogen, Carlsbad, CA, USA). The relative copy number of each transcript in each cDNA sample was measured using specific primers and iQ SYBR Green Supermix (Bio-Rad, Hercules, CA, USA) with a CFX96 real-time PCR detection system (Bio-Rad). The PCR cycling parameters were as follows: 3 min at 95°C, followed by 40 cycles of 10 sec at 95°C and 30 sec at the annealing temperatures of 55°C to 65°C suitable for each primer set. The target genes were selected based on the microarray data and β-actin (ACTB) was used as an internal control for normalization. The forward and reverse primers for FEZ1 were 5′-GGGACTGCATGAGAC CATGT-3′ and 5′-TTGAGGGCTGTAGCCAG ACT-3′, respectively. The forward and reverse primers for RNA binding motif protein 14 (RBM14) were 5′-GCAAAGAAGTGAAGGG CAAG-3′ and 5′-AAAGCCTGCTGGTAGTC GAA-3′, respectively. The forward and reverse primers for ACTB were 5′-CACACTGTGCC CATCTACGA-3′ and 5′-CCATCTCTTGCTC GAAGTCC-3′, respectively. Threshold cycles were measured for triplicate samples. A standard curve was constructed for each assay to adjust for differences in the amplification efficiency between primer sets. Differences in the abundance of target genes relative to ACTB among Li-treated samples (n = 6), VPA-treated samples (n = 6) and their non-treated controls (n = 6) were evaluated by one-way analysis of variance (ANOVA) followed by the Dunnett post-hoc test. Likewise, differences in target gene expression levels among CBZ-treated samples (n = 6), LTG-treated samples (n = 6), and their DMSO-treated controls (n = 6) were evaluated by ANOVA.

Western blotting

U-87 MG cells treated with mood stabilizers and control samples were homogenized in phosphate buffered saline (PBS) containing Triton X-100, 4-(2-hydroxyethyl)-1-piperazineethanesulfonic acid (HEPES), bovine serum albumin, gentamicin sulfate, and a proteinase inhibitor cocktail containing 4-(2-aminoethyl) benzenesulfonyl fluoride, aprotinin, leupeptin, bestatin, and pepstatin A (all from Sigma-Aldrich). The supernatant obtained after centrifugation (10,000 × *g* for 10 min at 4°C) was subjected to sodium dodecyl sulfate polyacrylamide gel electrophoresis (SDS-PAGE) and western blotting with the following primary antibodies: polyclonal goat anti-FEZ1 antibody (1:10000; Abcam, Cambridge, UK) and monoclonal mouse anti-ACTB antibody (1:10000; Sigma-Aldrich). The secondary antibodies employed were horseradish peroxidase-conjugated anti-goat IgG (1:2000; Dako, Glostrup, Denmark) and anti-mouse IgG (1:5000; Jackson ImmunoResearch, West Grove, PA, USA), respectively. Chemiluminescence was detected using an Amersham ECL Plus western blotting detection kit (GE Healthcare, Waukesha, WI, USA) and a LAS-1000 luminescence image analyzer (Fujifilm, Tokyo, Japan), and the results were quantified using ImageJ 1.42 software (http://rsb.info.nih.gov/ij/).

Immunostaining

FEZ1 protein has been shown to be preferentially expressed in neurons but not in astrocytes or oligodendrocytes in the rat brain (32). However, the expression of FEZ1 protein in human brain-derived cells has not been investigated. To determine the expression of FEZ1 proteins in human brain astrocyte cells (U-87 MG and ACBRI 371), neurons (SK-N-SH) and oligodendrocytes (OL)

were placed in a LAB-TEK glass 2-well (1×10^3 cells/well) chamber slide (Nunc, Rochester, NY, USA) together with 1 ml of the appropriate medium (MEM for U-87 MG, ACBRI 371, SK-N-SH; DMEM for OL) and incubated at 37°C, 5% CO_2 for six days. After fixation with ice-cold ethanol/acetone, cells were blocked in PBS containing 1% BSA (Sigma-Aldrich) and 10% normal horse serum (Dako) for 30 min at room temperature. After an overnight incubation at 4°C with primary antibodies, the cells were rinsed in PBS and then incubated at room temperature in the dark with secondary antibody. The primary antibodies used were as follows: polyclonal goat anti-FEZ1 antibody (1:5000; Abcam), polyclonal rabbit anti-GFAP antibody (1:200; Abcam) and monoclonal anti-NeuN antibody (1:200; Abcam). The corresponding secondary antibodies were as follows: Alexa Fluor 488 anti-goat IgG or Alex Fluor 594 anti-rabbit IgG (1:300; Invitrogen). Following incubation with the secondary antibody, the tissues were rinsed in PBS and subjected to nuclear staining with 4, 6-diamidino-2-phenylindole (DAPI) (Invitrogen). Microscopic images were captured using a Leica DAS Mikroskop microscope (Leica Microsystems, Wetzlar, Germany). To evaluate the effects of the four mood stabilizers on FEZ1 localization in U-87 MG cells, cells were cultured for five days with six different treatments (i.e., 1.2 mM Li, 1 mM VPA, 100 μM CBZ, 50 μM LTG, DMSO, and non-treated) in LAB-TEK chamber slides, and subjected to the above-mentioned immunostaining procedure.

Results

Microarray gene expression profiles

Among the 11,214 genes expressed in at least one of the 12 U-87 MG samples treated with or without mood stabilizers (6 types of media × 2 replicates = 12 samples), 65, 797, 315, and 641 genes were found to be induced with a fold change of > 1.2 (20% increase) by the Li, VPA, CBZ, and LTG treatments, respectively. In contrast, 142, 1008, 80, and 543 genes were suppressed with a fold change of < 0.833 (20% decrease) by the mood stabilizer treatments, respectively (Fig. 1). Tables 1 and 2 show gene symbols for the 10 most robustly up- and down-regulated genes in response to each mood stabilizer treatment, some of which have functions relevant to the mechanism of action of each mood stabilizer. VPA and LTG tended to affect more genes at the transcriptional level in astrocyte-derived cells, whereas the cellular effects

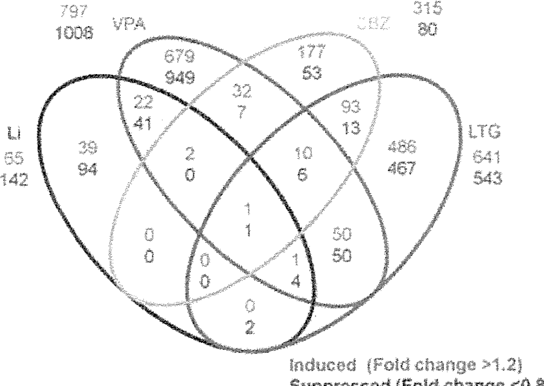

Fig. 1. Venn diagram summarizing the number of genes altered by each mood stabilizer and the overlaps among the genes altered by each mood stabilizer. Genes were selected according to the following criteria: a fold change > 1.2 (red) or < 0.83 (black) in both of the duplicated pairs of microarrays, a signal intensity > 20, and a detection p-value < 0.05 in all microarrays. Li = lithium; VPA = valproic acid; CBZ = carbamazepine; LTG = lamotrigine.

of the Li and CBZ treatments at the therapeutic concentrations used were relatively modest. Li and VPA commonly induced 26 genes and suppressed 46 genes, whereas Li demonstrated little overlap with the other anticonvulsants (3 induced genes and 1 suppressed gene in common between Li- and CBZ-treated samples; 2 induced and 7 suppressed genes in common between Li- and LTG-treated samples). The observed number of commonly regulated genes between Li- and VPA-treated samples was significantly higher than the expected number ($p < 0.001$). Furthermore, the observed number of commonly induced/suppressed genes between CBZ- and LTG-treated samples (104 and 20 genes, respectively) was also significantly higher than the expected number ($p < 0.001$). Hierarchical clustering analysis of the signal intensity ratio of mood-stabilizer-treated cells divided the four mood stabilizers into two groups, Li-VPA and CBZ-LTG (Fig. 2), which was consistent with the numbers of overlapping genes among the four mood stabilizers.

Induction of FEZ1 expression in human astrocytic cells

FEZ1 was the only gene induced by all four mood stabilizers. The microarray data revealed that the FEZ1 mRNA expression level was increased by 34%, 119%, 35%, and 115% after treatment with Li, VPA, CBZ, and LTG, respectively (Fig. 3A). FEZ1 was the top 5th, 141st, 193rd, and 10th most highly expressed gene among the total genes induced by Li, VPA, CBZ, and LTG, respectively (Table 1).

Table 1. The 10 most induced genes in response to each mood stabilizer

	Lithium			Valproic acid			Carbamazepine			Lamotrigine		
Rank	Symbol	Fold change	Function	Symbol	Fold change	Function	Symbol	Fold change	Function	Symbol	Fold change	Function
1	MMP14	1.40	Proteolysis	TSPAN7	5.05	Glycosylation	KIAA1033	1.91	Uncharacterized	PAIP1	2.00	RNA stabilization
2	RASIP1	1.37	Uncharacterized	CA2	3.55	One-carbon metabolism	NIPBL	1.83	Cell cycle	DNAJC10	1.87	Protein folding
3	C21orf70	1.33	Uncharacterized	LRRN3	3.33	Activation of MAPK activity	PAIP1	1.61	RNA stabilization	TUBG1	1.78	Cytoskeleton organization
4	FABP4	1.32	Proliferation	GABRB1	3.30	Ion channel complex	POLH	1.60	DNA repair	CUTA	1.76	Protein complex assembly
5	FEZ1	1.32	Cell motion/ axon guidance	GAP43	3.28	Cell motion/ axon guidance	AS3MT	1.54	Xenobiotic metabolism	KIAA1033	1.73	Uncharacterized
6	AAMP	1.31	Cell motion	ASAP3	3.20	Small GTPase signaling	ZKSCAN4	1.52	Transcription	MMP1	1.71	Proteolysis
7	LENG8	1.30	Uncharacterized	TNFAIP6	3.02	Cell adhesion	ERMN	1.52	Cytoskeleton organization	DDX59	1.70	Uncharacterized
8	MYCL1	1.30	Regulation of transcription	VGF	2.91	Cell-cell signaling	FAR1	1.50	Fatty acid metabolism	CSNK1A1	1.67	Wnt signaling
9	CRB2	1.30	Sensory perception	BIRC3	2.91	Anti-apoptosis	MAP3K2	1.50	Activation of MAPK activity	UBE4A	1.66	Proteolysis
10	NDUFB1	1.29	Oxidative phosphorylation	SPINK13	2.88	Uncharacterized	KPNA5	1.50	Intracellular protein transport	FEZ1	1.64	Cell motion/ axon guidance

The table shows the 10 most robust fold changes in the signal intensities of the mood-stabilizer-treated samples divided by the appropriate control samples. Each fold change represents the minimal value among the fold changes determined in four comparisons between duplicate mood-stabilizer-treated samples and duplicate control samples. Columns labeled *Function* indicate representative *biological process* categories from the Gene Ontology database (http://www.geneontology.org/) to which each gene belongs.

Table 2. The 10 most suppressed genes in response to each mood stabilizer

	Lithium			**Valproic acid**			**Carbamazepine**			**Lamotrigine**		
Rank	Symbol	Fold change	Function	Symbol	Fold change	Function	Symbol	Fold change	Function	Symbol	Fold change	Function
1	AFMID	0.63	Tryptophan metabolism	CA9	0.22	One-carbon metabolism	RBM14	0.67	Transcription	ABCD1	0.47	Fatty acid metabolism
2	RBM14	0.65	Transcription	ZP1	0.23	Fertilization	PUS1	0.71	RNA processing	NFIC	0.52	Transcription
3	RIMBP3	0.65	Uncharacterized	KCNS1	0.28	Ion transport	CLIP1	0.73	Cell cycle	PPDPF	0.59	Uncharacterized
4	RAPGEFL1	0.66	Small GTPase signaling	CHI3L2	0.31	Polysaccharide metabolism	HSP90AA1	0.74	Protein folding	ATN1	0.61	Cell death
5	SNORD14A	0.68	Uncharacterized	SERP2	0.32	Protein transport	CDK5RAP3	0.75	Cell cycle	SMARCC2	0.61	Chromatin organization
6	SETD7	0.68	Chromatin organization	OLFML3	0.33	Uncharacterized	AKIRIN1	0.76	Uncharacterized	JOSD2	0.61	Uncharacterized
7	P2RY6	0.68	Ion transport	SLC2A1	0.34	Monosaccharide transport	MAP2K3	0.76	Activation of MAPK activity	SOLH	0.61	Proteolysis
8	ZNF200	0.70	Zinc ion binding	TSPAN10	0.35	Uncharacterized	HIST2H2BF	0.77	Chromatin organization	IFITM3	0.63	Immune response
9	DOCK3	0.71	Uncharacterized	ARTN	0.35	Cell proliferation	CPT1B	0.77	Fatty acid metabolism	SLN	0.63	Calcium ion transport
10	COL4A3BP	0.72	Cell morphogenesis	C10orf10	0.35	Uncharacterized	CTSL1	0.77	Proteolysis	AHDC1	0.63	Uncharacterized

The table shows the 10 least robust fold changes in the signal intensities of the mood-stabilizer-treated samples divided by the appropriate control samples. Each fold change represents the maximal value among the fold changes determined in four comparisons between duplicate mood-stabilizer-treated samples and duplicate control samples. Columns labeled *Function* indicate representative *biological process* categories from the Gene Ontology database (http://www.geneontology.org/) to which each gene belongs.

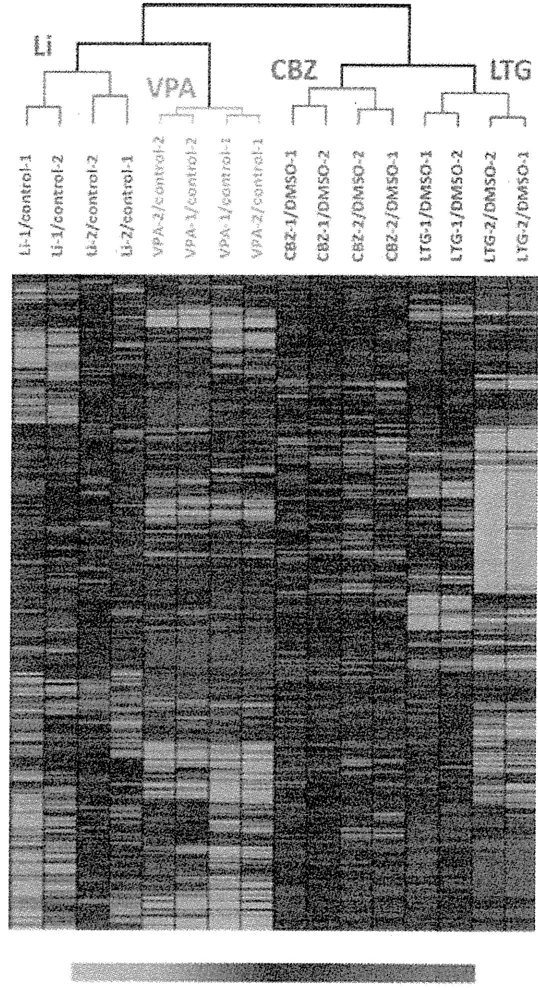

Fig. 2. Hierarchical clustering of gene expression changes caused by the mood stabilizers. Log_2-transformed ratios of the signal intensities of samples treated with mood stabilizers to the signal intensities of their controls [lithium (Li)-treated sample/non-treated control, valproic acid (VPA)-treated sample/non-treated control, carbamazepine (CBZ)-treated sample/DMSO-treated control, lamotrigine (LTG)-treated sample/DMSO-treated control] were subjected to an average linkage hierarchical clustering analysis. Ratios for each of the four combinations of duplicate drug-treated samples to their duplicate control samples were calculated.

Verification by qRT-PCR using six independent cell cultures for each mood stabilizer treatment and for the control samples showed that the FEZ1 mRNA levels were significantly increased by 49% ($p < 0.05$), 78% ($p < 0.001$), 42% ($p < 0.01$), and 47% ($p < 0.001$) following treatment with Li (0.75 mM), VPA (0.5 mM), CBZ (50 μM), and LTG (5 μM) (Fig. 3A), respectively. Western blotting analysis demonstrated that the VPA and LTG treatments significantly induced FEZ1 protein expression levels by 36% ($p < 0.05$) and 60% ($p < 0.01$), respectively, at the lower concentrations (0.5 mM and 5 μM, respectively) (Fig. 3B), while neither Li nor CBZ treatment significantly altered FEZ1 protein expression levels at lower concentrations (0.75 mM and 50 μM, respectively). On the other hand, FEZ1 protein expression levels were significantly increased by 42% ($p < 0.05$), 58% ($p < 0.05$), 75% ($p < 0.01$), and 62% ($p < 0.01$) following treatment with the higher concentrations of Li (1.2 mM), VPA (1 mM), CBZ (100 μM), and LTG (50 μM), respectively (Fig. 3C).

Suppression of RBM14 expression in human astrocytic cells

RBM14 was the only gene suppressed by all four mood stabilizers. The microarray data showed that RBM14 was decreased by 39%, 65%, 33%, and 54% following treatment with Li, VPA, CBZ, and LTG, respectively (Fig. 3D). RBM14 was the top 2nd, 808th, 1st, and 146th most robustly downregulated gene among the total genes suppressed by Li, VPA, CBZ, and LTG, respectively (Table 2). qRT-PCR analysis revealed that the mRNA levels of RBM14 were decreased by 37% ($p < 0.001$), 47% ($p < 0.05$), 32% ($p < 0.05$), and 36% ($p < 0.05$) following treatment with Li, VPA, CBZ, and LTG, respectively (Fig. 3D). However, the protein expression levels of RBM14 were not altered in response to any of the mood stabilizer treatments at any of the tested doses (Fig. 3E).

Intracellular localization of FEZ1 in human brain-derived cells

To assess FEZ1 protein expression in human brain-derived cells, the human astrocyte-derived cell line U-87 MG, the human primary astrocyte cells ACBRI 371, the human neuron-derived cell line SK-N-SH, and the human oligodendrocyte-derived cell line OL, the cultures were subjected to immunofluorescent staining with anti-FEZ1 antibody (red) and anti-GFAP (green) or anti-NeuN (green) antibodies. The cell nuclei were stained with 4′, 6-diamidino-2-phenylindole (DAPI, blue) and observed under UV excitation. The immunostaining images revealed FEZ1 protein expression in the U-87 MG (Figs. 4A–C), ACBRI 371 (Figs. 4D–F), and SK-N-SH (Figs. 4G–I) cells, but not in OL cells (data not shown). The FEZ1 immunostaining signal was localized in the cytoplasm of human astrocyte- and neuron-derived cells, while the nuclei were immunonegative (arrowheads). There were no differences in intracellular FEZ1 localization in U-87 MG cells after five days of treatment with Li, VPA, CBZ, and LTG (data not shown).

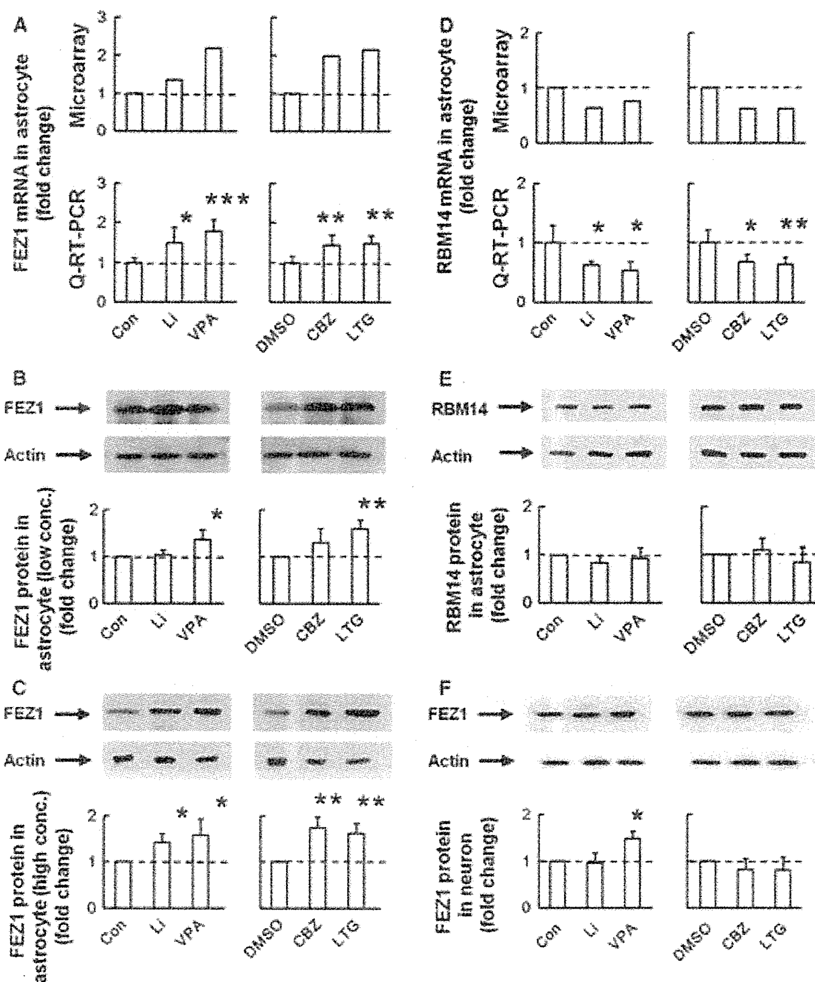

Fig. 3. Transcriptional and protein expression levels of fasciculation and elongation protein zeta 1 (FEZ1) and RNA binding motif protein 14 (RBM14) in astrocytic and neuronal cells after the mood stabilizer treatments. (**A**) The upper bar graph shows the FEZ1 transcript signal intensities determined from microarray analyses of human astrocyte-derived cells, relative to the averaged signal intensity of the control samples. The lower bar graph shows the FEZ1 transcript levels in human astrocyte-derived cells relative to the averaged signal intensity of the control samples, as measured by qRT-PCR analysis. (**B**) Gel images and bar graph of the signal intensities determined by western blotting of human astrocyte-derived cells using anti-FEZ1 antibody, after treatment with the lower concentrations of the four mood stabilizers [0.75 mM lithium (Li), 0.5 mM valproic acid (VPA), 50 μM carbamazepine (CBZ), and 5 μM lamotrigine (LTG)], relative to the averaged signal intensity of the control samples. (**C**) Gel images and bar graph of the signal intensities determined by western blotting of human astrocyte-derived cells using anti-FEZ1 antibody, after treatment with the higher concentrations of the four mood stabilizers (1.2 mM Li, 1 mM VPA, 100 μM CBZ, and 50 μM LTG), relative to the averaged signal intensity of the control samples. (**D**) The upper bar graph shows the signal intensities for the RBM14 transcript from microarray analyses of human astrocyte-derived cells relative to the averaged signal intensity of the control samples. The lower bar graph shows the transcript levels of RBM14 in human astrocyte-derived cells relative to the averaged signal intensity of the control samples, as measured by qRT-PCR analysis. (**E**) Gel images and bar graph of the signal intensities determined by western blotting of human astrocyte-derived cells using anti-RBM14 antibody, after treatment with the higher concentrations of the four mood stabilizers (1.2 mM Li, 1 mM VPA, 100 μM CBZ, and 50 μM LTG), relative to the averaged signal intensity of the control samples. (**F**) Gel images and bar graph of the signal intensities determined by western blotting of human neuron-derived cells using anti-FEZ1 antibody, after treatment with the higher concentrations of the four mood stabilizers (1.2 mM Li, 1 mM VPA, 100 μM CBZ, and 50 μM LTG), relative to the averaged signal intensity of the control samples. Con = non-treated control; DMSO = dimethyl sulfoxide-treated control. *$p < 0.05$; **$p < 0.01$; ***$p < 0.001$.

Effect of mood stabilizers on FEZ1 expression in human neuronal cells

To determine whether any of the mood stabilizers affected FEZ1 protein expression levels in human neuron-derived cells, human neuron-derived SK-N-SH cells were subjected to mood stabilizer treatments in the same manner employed for the U-87 MG experiments. Treatments with any of the four mood stabilizers at the lower

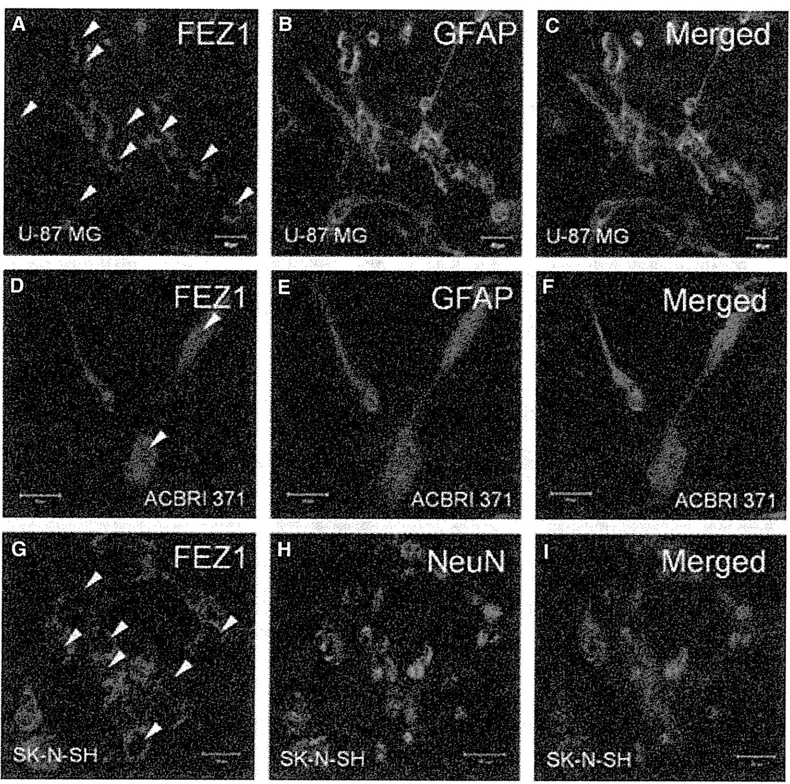

Fig. 4. Intracellular localization of fasciculation and elongation protein zeta 1 (FEZ1) protein in human astrocytic and neuronal cells. Figures A, B, and C show the intracellular localization of FEZ1 protein (**A**), glial fibrillary acidic protein (GFAP), an astrocyte marker (**B**), and the merged image showing the distribution of FEZ1 and GFAP (**C**) in the human astrocyte-derived cell line U-87 MG (scale bar: 40 μm). D, E, and F show the intracellular localization of FEZ1 protein (**D**), GFAP protein (**E**), and the merged image showing the distribution of FEZ1 and GFAP (**F**) in the human primary astrocyte cell culture ACBRI371 (scale bar: 40 μm). Figures G, H, and I show the intracellular localization of FEZ1 protein (**G**), the neuronal specific nuclear protein (NeuN) (**H**), and the merged image showing the distribution of FEZ1 and NeuN (**I**) in the human neuron-derived cell line SK-N-SH (scale bar: 20 μm). Cell nuclei were stained with 4′,6-diamidino-2-phenylindole (DAPI, blue) (C, F, I). Arrow heads indicate nuclei of cells lacking FEZ1 signal.

concentrations did not alter FEZ1 protein expression levels in SK-N-SH cells (data not shown). Following treatment with the mood stabilizers at the high concentrations, only VPA increased the FEZ1 protein expression level in SK-N-SH cells (Fig. 3F).

Discussion

Among the four mood stabilizers, VPA affected the expression of the largest numbers of genes. VPA may exert its effect on transcriptional regulation by inhibiting histone deacetylase (HDAC) activity (33, 34); however, it remains uncertain whether the strong effect of VPA on transcriptional regulation is relevant to its mood-stabilizing effect and/or HDAC inhibition-mediated teratogenesis (35). It is interesting that LTG also affects a relatively large number of genes, despite the use of a concentration of LTG in the microarray experiments that was close to the lower limit of its therapeutic range (36, 37). LTG may have unknown mechanisms of action that are relevant to its potent effect on transcriptional regulation.

The clustering analysis suggested that Li and VPA regulated the transcriptional activities of a common set of genes, whereas CBZ with LTG affected a different set of genes. Li and VPA have been reported to share common molecular mechanisms of action, including effects on glycogen synthase kinase 3β (38, 39) and phosphatidylinositol (40) signaling, which may underlie the common effects of Li and VPA on transcriptional regulation in U-87 MG cells. CBZ and LTG may share other unknown mechanisms which cause the observed transcriptional alterations in astrocytes.

Interestingly, only VPA increased FEZ1 protein expression in a neuron-derived cell line at a concentration representing the higher limit of the therapeutic range, while Li, CBZ, and LTG did not induce FEZ1 protein expression in neuronal cells at any concentration. The FEZ1 gene has been functionally characterized in the rodent brain and

a human neuron-derived cell line (41). These rodent studies have indicated that FEZ1 is preferentially expressed in neuronal cells and involved in normal axonal bundling, elongation within axon bundles of neurons, transport of intracellular components (including mitochondria), and release of neurotransmitters (32, 42, 43). FEZ1 protein is phosphorylated by PKCζ and then translocated from the cytoplasmic membrane to the cytoplasm, where it induces axonal growth and neuronal differentiation (44). FEZ1 protein has also been reported to localize to growth cones and associate with F-actin in SK-N-SH cells and cultured hippocampal neurons (41). Although the mechanism underlying its transcriptional regulation requires further investigation, induction of FEZ1 protein in neuronal cells by VPA might contribute to axonal bundling, transport of intracellular components, and neurotransmitter release.

The most intriguing finding of the genome-wide expression analysis of mood-stabilizer-treated U-87 MG cells was that only the FEZ1 and RBM14 transcripts were substantially induced and suppressed by all four mood stabilizers. The significant induction of FEZ1 molecules at both the transcript and the protein levels was verified by qRT-PCR and western blotting. Although FEZ1 transcript levels were significantly increased by the four mood stabilizers at lower concentrations, protein levels increased only at higher Li and CBZ concentrations. In general, changes in protein levels depend on levels of the transcript, translation efficiency, and degradation of the existing protein (45). Although the modest increase in FEZ1 transcripts after Li and CBZ treatments at lower concentrations may not be sufficient to yield a corresponding increase in FEZ1 translation, it implies that higher doses of Li and CBZ may increase transcript levels to a degree that allows for increased FEZ1 translation. Mood stabilizers might somehow affect translation efficiency and degradation of the existing protein as well, although these possibilities were not addressed in this study.

In addition to neuronal cells, FEZ1 is expressed in cultured rat neonatal astrocytes (46); however, it is expressed at barely detectable levels in adult astrocytes and oligodendrocytes (32). In our experiments, unlike the previous adult rodent studies, FEZ1 protein was expressed in the cytoplasm of both transformed and primary astrocytes, as well as in neuronal cells from the human adult brain, while it was not detectable in the human oligodendrocyte cell line (data not shown). No differences were detected in the intracellular distribution pattern of the FEZ1 protein between the human astrocytic and neuronal cells.

In general, the transcription of genes in certain cell types can vary among species. One example of this is the transcriptional regulation of toll-like receptors and nitric oxide synthase 2 in humans and rodents (47, 48). While exons 2-10 of human FEZ1 and rodent Fez1 are highly homologous (mouse: 90%, rat: 91%), exon 1 and the promoter region are not. This difference in the promoter region may underlie the expression of the gene in human astrocytes, but its absence in rodents.

Astrocytes are compact round cells in the early developmental stages, and subsequently, they project highly branched cellular processes that form connections with other cell types or with brain structures, similar to the extension of axons and dendrites observed in neurons. The localization of FEZ1 proteins suggests that FEZ1 may be involved in the extension and maintenance of astrocyte processes, mitochondrial functions, and the development and maintenance of structural formations in astrocytes; however, the function of FEZ1 protein in astrocytes requires further investigation.

Although there are reports that FEZ1 transcripts are decreased in postmortem brain tissue of patients with schizophrenia (49) and that FEZ1 and schizophrenia are modestly associated (50), neither postmortem brain studies nor genetic association studies targeting FEZ1 have been reported. However, indirect evidence from animal models and cell culture studies suggests the possible involvement of FEZ1 dysfunction in the pathogenesis of BD. To this end, FEZ1 knockout mice are hypersensitive to psychostimulant treatment (51), which suggests that hypofunction of FEZ1 may contribute to hyperdopaminergic conditions which have been implicated in the pathogenesis of the manic state of BD (52). In addition, FEZ1 has been reported to play an important role in the establishment of neuronal polarity by controlling the axonal transport of mitochondria (53, 54). Thus, an impairment of FEZ1 might be involved in the mitochondrial dysfunction implicated in BD (55, 56). Further studies will be needed to investigate abnormalities in FEZ1 expression and function in postmortem brains of BD subjects.

Our finding that four widely prescribed mood stabilizers commonly induced FEZ1 protein expression in astrocyte-derived cells raises the question of what the link is between the mechanisms of action of the mood stabilizers and FEZ1 induction. It is also unclear whether FEZ1 induction is specific to these mood stabilizers, and whether this induction is involved in the mood-stabilizing effects of these drugs. Further studies

will be needed to address these issues and the involvement of FEZ1 in the pathogenesis of BD.

Although the RBM14 transcript was suppressed by the mood stabilizer treatments, RBM14 protein expression was not affected by any of the mood stabilizers. While protein levels generally correlate with transcript levels, there can be discrepancies due to variability in translation efficiency and protein degradation (45). Thus, RBM14 translation efficiency may have increased or RBM14 degradation may have decreased in parallel with the decrease in RBM14 transcripts. Since RBM14 exerts its cellular effects by encoding the coactivator activator (CoAA) protein (57), the suppression of RBM14 transcripts may not be directly relevant to the mechanism of action of mood stabilizers. However, there remains the possibility that decreases in RBM14 transcripts may influence cellular function by modulating the expression of other transcripts.

Besides the genes commonly altered by the four mood stabilizers, each mood stabilizer uniquely altered the expression of certain genes with robust fold changes as shown in Tables 1 and 2. Although further studies will be needed to characterize the function of these regulated genes and their roles in mood stabilization, previous studies have suggested the possible involvement of some of these genes in the mechanism of action of the respective mood stabilizer. For example, VPA induced gamma-aminobutyric acid A receptor, beta 1 (GABRB1) and growth associated protein 43 (GAP43) transcripts by 330% and 328%, respectively (Table 1). GABA A receptor is expressed in both astrocytes and neurons. The GABA A receptor is thought to transfer signals from inhibitory interneurons to adjacent glial cells, and may regulate extracellular Cl^- concentrations in the vicinity of a GABAergic synapse (58). The SPECT study showed that levels of GABA A receptors were decreased in the sensory motor cortex of mood disorder patients with akinetic catatonia (59), whereas GABA receptors were increased in the rodent hippocampus after VPA treatment (60). These disease-related or VPA-induced alterations in GABA receptor expression may, at least in part, reflect the expression of GABA A receptors in astrocytes.

VPA was previously reported to increase neuronal GAP43 and cell survival *in vitro* (61). The present study demonstrated that VPA also induces GAP43 in astrocytes. Although GAP43 is a calmodulin-binding phosphoprotein primarily found in neuronal growth cones and is an intrinsic presynaptic determinant for neurite outgrowth and plasticity (62), it is also expressed in astrocytes, in particular type 2 astrocytes (63, 64). One study reported that ischemic injury induces GAP43 expression in reactive astrocytes, which protect the brain from ischemic injury by normalizing extracellular fluid H^+ or glutamate levels, or by releasing neuronal growth factors (65, 66). Given that postmortem brain studies have shown that GAP43 expression is significantly reduced in the anterior cingulate cortex of BD patients (67) and the prefrontal cortex of depressed suicide victims (68), VPA might exert its effects by inducing GAP43 levels.

DNA polymerase eta (POLH) increased by 60% after CBZ treatment, whereas interferon-induced transmembrane protein 3 (IFITM3) decreased by 37% after LTG treatment (Tables 1 and 2). Postmortem brain microarray analyses showed that POLH expression was decreased in the hippocampal CA1 region (69), and IFITM3 was increased in the prefrontal cortex of BD patients (70). This suggests the possibility that CBZ-induced POLH expression and LTG-mediated IFITM3 suppression may normalize the altered levels of these genes in affected brains. Thus, transcriptional regulation may underlie the mood-stabilizing actions of these drugs.

In conclusion, the microarray data obtained for human astrocytic cells identified FEZ1 as a gene that is commonly induced by the four mood stabilizers, Li, VPA, CBZ, and LTG. Unlike the studies performed in rodents, in the present study FEZ1 was expressed in the cytoplasm of human astrocytic cells and neuronal cells. Our data suggest that FEZ1 may play important roles in human astrocytes, and that mood stabilizers might exert their cytoprotective and mood-stabilizing effects via FEZ1 induction in astrocytes. Further studies will be needed to address the involvement of FEZ1 in the mechanisms of action of mood stabilizers and the pathogenesis of BD.

Acknowledgements

This work was supported by a grant-in-aid for scientific research (B) (no. 19390300) from the Ministry of Education, Culture, Sports, Science, and Technology of Japan, a grant-in-aid from the Japan Research Foundation for Clinical Pharmacology, and the Intramural Research Grant (21-6) for Neurological and Psychiatric Disorders from the National Center of Neurology and Psychiatry. We appreciate the assistance of Ms. Yoshie Kikuchi (Tohoku University) for the technical contributions in cell culture and qRT-PCR experiments.

References

1. Williams R, Ryves WJ, Dalton EC et al. A molecular cell biology of lithium. Biochem Soc Trans 2004; 32: 799–802.

2. Di Daniel E, Cheng L, Maycox PR, Mudge AW. The common inositol-reversible effect of mood stabilizers on neurons does not involve GSK3 inhibition, myo-inositol-1-phosphate synthase or the sodium-dependent myo-inositol transporters. Mol Cell Neurosci 2006; 32: 27–36.
3. Beaulieu JM, Caron MG. Looking at lithium: molecular moods and complex behaviour. Mol Interv 2008; 8: 230–241.
4. O'Brien WT, Klein PS. Validating GSK3 as an in vivo target of lithium action. Biochem Soc Trans 2009; 37: 1133–1138.
5. Quiroz JA, Gould TD, Manji HK. Molecular effects of lithium. Mol Interv 2004; 4: 259–272.
6. Shaltiel G, Dalton EC, Belmaker RH, Harwood AJ, Agam G. Specificity of mood stabilizer action on neuronal growth cones. Bipolar Disord 2007; 9: 281–289.
7. Leng Y, Liang MH, Ren M, Marinova Z, Leeds P, Chuang DM. Synergistic neuroprotective effects of lithium and valproic acid or other histone deacetylase inhibitors in neurons: roles of glycogen synthase kinase-3 inhibition. J Neurosci 2008; 28: 2576–2588.
8. Du J, Gray NA, Falke C, Yuan P, Szabo S, Manji HK. Structurally dissimilar antimanic agents modulate synaptic plasticity by regulating AMPA glutamate receptor subunit GluR1 synaptic expression. Ann NY Acad Sci 2003; 1003: 378–380.
9. Friedrich MJ. Molecular studies probe bipolar disorder. JAMA 2005; 293: 535–536.
10. Doetsch F, Caillé I, Lim DA, García-Verdugo JM, Alvarez-Buylla A. Subventricular zone astrocytes are neural stem cells in the adult mammalian brain. Cell 1999; 97: 703–716.
11. Hama K, Arii T, Kosaka T. Three-dimensional organization of neuronal and glial processes: high voltage electron microscopy. Microsc Res Tech 1994; 29: 357–367.
12. Haydon PG. GLIA: listening and talking to the synapse. Nat Rev Neurosci 2001; 2: 185–193.
13. Kosaka T, Hama K. Three-dimensional structure of astrocytes in the rat dentate gyrus. J Comp Neurol 1986; 249: 242–260.
14. Ventura R, Harris KM. Three-dimensional relationships between hippocampal synapses and astrocytes. J Neurosci 1999; 19: 6897–6906.
15. Rajkowska G. Cell pathology in bipolar disorder. Bipolar Disord 2002; 4: 105–116.
16. Ongür D, Drevets WC, Price JL. Glial reduction in the subgenual prefrontal cortex in mood disorders. Proc Natl Acad Sci USA 1998; 95: 13290–13295.
17. Rajkowska G, Halaris A, Selemon LD. Reductions in neuronal and glial density characterize the dorsolateral prefrontal cortex in bipolar disorder. Biol Psychiatry 2001; 49: 741–752.
18. Manji HK, Moore GJ, Rajkowska G, Chen G. Neuroplasticity and cellular resilience in mood disorders. Mol Psychiatry 2000; 5: 578–593.
19. Webster MJ, O'Grady J, Kleinman JE, Weickert CS. Glial fibrillary acidic protein mRNA levels in the cingulate cortex of individuals with depression, bipolar disorder and schizophrenia. Neuroscience 2005; 133: 453–461.
20. Johnston-Wilson NL, Sims CD, Hofmann JP et al. Disease-specific alterations in frontal cortex brain proteins in schizophrenia, bipolar disorder, and major depressive disorder. The Stanley Neuropathology Consortium. Mol Psychiatry 2000; 5: 142–149.
21. Andreazza AC, Cassini C, Rosa AR et al. Serum S100B and antioxidant enzymes in bipolar patients. J Psychiatr Res 2007; 41: 523–529.
22. Roche S, Cassidy F, Zhao C et al. Candidate gene analysis of 21q22: support for S100B as a susceptibility gene for bipolar affective disorder with psychosis. Am J Med Genet B Neuropsychiatr Genet 2007; 144B: 1094–1096.
23. Pardo R, Andreolotti AG, Ramos B, Picatoste F, Claro E. Opposed effects of lithium on the MEK-ERK pathway in neural cells: inhibition in astrocytes and stimulation in neurons by GSK3 independent mechanisms. J Neurochem 2003; 87: 417–426.
24. Chen PS, Peng GS, Li G et al. Valproate protects dopaminergic neurons in midbrain neuron/glia cultures by stimulating the release of neurotrophic factors from astrocytes. Mol Psychiatry 2006; 11: 1116–1125.
25. Lubrich B, van Calker D. Inhibition of the high affinity myo-inositol transport system: a common mechanism of action of antibipolar drugs? Neuropsychopharmacology 1999; 21: 519–529.
26. Li B, Zhang S, Li M, Zhang H, Hertz L, Peng L. Down-regulation of GluK2 kainate receptor expression by chronic treatment with mood-stabilizing anti-convulsants or lithium in cultured astrocytes and brain, but not in neurons. Neuropharmacology 2009; 57: 375–385.
27. Li B, Zhang S, Li M, Hertz L, Peng L. Chronic treatment of astrocytes with therapeutically relevant fluoxetine concentrations enhances cPLA2 expression secondary to 5-HT2B-induced, transactivation-mediated ERK1/2 phosphorylation. Psychopharmacology 2009; 207: 1–12.
28. Song D, Du T, Li B et al. Astrocytic alkalinization by therapeutically relevant lithium concentrations: implications for myo-inositol depletion. Psychopharmacology 2008; 200: 187–195.
29. Dahlquist KD, Salomonis N, Vranizan K, Lawlor SC, Conklin BR. GenMAPP, a new tool for viewing and analyzing microarray data on biological pathways. Nat Genet 2002; 31: 19–20.
30. Miller LD, Long PM, Wong L, Mukherjee S, McShane LM, Liu ET. Optimal gene expression analysis by microarrays. Cancer Cell 2002; 2: 353–361.
31. Choe SE, Boutros M, Michelson AM, Church GM, Halfon MS. Preferred analysis methods for Affymetrix GeneChips revealed by a wholly defined control dataset. Genome Biol 2005; 6: R16.
32. Honda A, Miyoshi K, Baba K et al. Expression of fasciculation and elongation protein zeta-1 (FEZ1) in the developing rat brain. Brain Res Mol Brain Res 2004; 122: 89–92.
33. Busa WB, Gimlich RL. Lithium-induced teratogenesis in frog embryos prevented by a polyphosphoinositide cycle intermediate or a diacylglycerol analog. Dev Biol 1989; 132: 315–324.
34. Phiel CJ, Zhang F, Huang EY, Guenther MG, Lazar MA, Klein PS. Histone deacetylase is a direct target of valproic acid, a potent anticonvulsant, mood stabilizer, and teratogen. J Biol Chem 2001; 276: 36734–36741.
35. Gurvich N, Berman MG, Wittner BS, Gentleman RC, Klein PS, Green JB. Association of valproate-induced teratogenesis with histone deacetylase inhibition in vivo. FASEB J 2005; 19: 1166–1168.
36. May TW, Rambeck B, Jurgens U. Serum concentrations of lamotrigine in epileptic patients: the influence of dose and comedication. Ther Drug Monit 1996; 18: 523–531.
37. Fraser AD, MacNeil W, Isner AF, Camfield PR. Lamotrigine analysis in serum by high-performance liquid chromatography. Ther Drug Monit 1995; 17: 174–178.
38. Chen G, Huang LD, Jiang YM, Manji HK. The mood-stabilizing agent valproate inhibits the activity of glycogen synthase kinase-3. J Neurochem 1999; 72: 1327–1330.

39. De Sarno P, Li X, Jope RS. Regulation of Akt and glycogen synthase kinase-3 beta phosphorylation by sodium valproate and lithium. Neuropharmacology 2002; 43: 1158–1164.
40. Williams RS, Cheng L, Mudge AW, Harwood AJ. A common mechanism of action for three mood-stabilizing drugs. Nature 2002; 417: 292–295.
41. Miyoshi K, Honda A, Baba K et al. Disrupted-In-Schizophrenia 1, a candidate gene for schizophrenia, participates in neurite outgrowth. Mol Psychiatry 2003; 8: 685–694.
42. Bloom L, Horvitz HR. The Caenorhabditis elegans gene unc-76 and its human homologs define a new gene family involved in axonal outgrowth and fasciculation. Proc Natl Acad Sci USA 1997; 94: 3414–3419.
43. Assmann EM, Alborghetti MR, Camargo ME, Kobarg J. FEZ1 dimerization and interaction with transcription regulatory proteins involves its coiled-coil region. J Biol Chem 2006; 281: 9869–9881.
44. Kuroda S, Nakagawa N, Tokunaga C, Tatematsu K, Tanizawa K. Mammalian homologue of the Caenorhabditis elegans UNC-76 protein involved in axonal outgrowth is a protein kinase C zeta-interacting protein. J Cell Biol 1999; 144: 403–411.
45. de Sousa Abreu R, Penalva LO, Marcotte EM, Vogel C. Global signatures of protein and mRNA expression levels. Mol Biosyst 2009; 5: 1512–1526.
46. He J, Liu J, Zhang Z, Sun M, Zhu T, Xia C. Expression of fasciculation and elongation protein zeta-1 (FEZ1) in cultured rat neonatal astrocytes. Mol Cell Biochem 2009; 325: 159–167.
47. Rehli M. Of mice and men: species variations of Toll-like receptor expression. Trends Immunol 2002; 23: 375–378.
48. Rico D, Vaquerizas JM, Dopazo H, Bosca L. Identification of conserved domains in the promoter regions of nitric oxide synthase 2: implications for the species-specific transcription and evolutionary differences. BMC Genomics 2007; 8: 271.
49. Lipska BK, Peters T, Hyde TM et al. Expression of DISC1 binding partners is reduced in schizophrenia and associated with DISC1 SNPs. Hum Mol Genet 2006; 15: 1245–1258.
50. Yamada K, Nakamura K, Minabe Y et al. Association analysis of FEZ1 variants with schizophrenia in Japanese cohorts. Biol Psychiatry 2004; 56: 683–690.
51. Sakae N, Yamasaki N, Kitaichi K et al. Mice lacking the schizophrenia-associated protein FEZ1 manifest hyperactivity and enhanced responsiveness to psychostimulants. Hum Mol Genet 2008; 17: 3191–3203.
52. Cousins DA, Butts K, Young AH. The role of dopamine in bipolar disorder. Bipolar Disord 2009; 11: 787–806.
53. Fujita T, Maturana AD, Ikuta J et al. Axonal guidance protein FEZ1 associates with tubulin and kinesin motor protein to transport mitochondria in neurites of NGF-stimulated PC12 cells. Biochem Biophys Res Commun 2007; 361: 605–610.
54. Ikuta J, Maturana A, Fujita T et al. Fasciculation and elongation protein zeta-1 (FEZ1) participates in the polarization of hippocampal neuron by controlling the mitochondrial motility. Biochem Biophys Res Commun 2007; 353: 127–132.
55. Kato T. The role of mitochondrial dysfunction in bipolar disorder. Drug News Perspect 2006; 19: 597–602.
56. Quiroz JA, Gray NA, Kato T, Manji HK. Mitochondrially mediated plasticity in the pathophysiology and treatment of bipolar disorder. Neuropsychopharmacology 2008; 33: 2551–2565.
57. Auboeuf D, Dowhan DH, Li X et al. CoAA, a nuclear receptor coactivator protein at the interface of transcriptional coactivation and RNA splicing. Mol Cell Biol 2004; 24: 442–453.
58. MacVicar BA, Tse FW, Crichton SA, Kettenmann H. GABA-activated Cl- channels in astrocytes of hippocampal slices. J Neurosci 1989; 9: 3577–3583.
59. Northoff G, Steinke R, Czcervenka C et al. Decreased density of GABA-A receptors in the left sensorimotor cortex in akinetic catatonia: investigation of in vivo benzodiazepine receptor binding. J Neurol Neurosurg Psychiatry 1999; 67: 445–450.
60. Motohashi N. GABA receptor alterations after chronic lithium administration. Comparison with carbamazepine and sodium valproate. Prog Neuropsychopharmacol Biol Psychiatry 1992; 16: 571–579.
61. Yuan PX, Huang LD, Jiang YM, Gutkind JS, Manji HK, Chen G. The mood stabilizer valproic acid activates mitogen-activated protein kinases and promotes neurite growth. J Biol Chem 2001; 276: 31674–31683.
62. Aigner L, Arber S, Kapfhammer JP et al. Overexpression of the neural growth-associated protein GAP-43 induces nerve sprouting in the adult nervous system of transgenic mice. Cell 1995; 83: 269–278.
63. da Cunha A, Vitković L. Regulation of immunoreactive GAP-43 expression in rat cortical macroglia is cell type specific. J Cell Biol 1990; 111: 209–215.
64. Vitković L, Steisslinger HW, Aloyo VJ, Mersel M. The 43-kDa neuronal growth-associated protein (GAP-43) is present in plasma membranes of rat astrocytes. Proc Natl Acad Sci USA 1988; 85: 8296–8300.
65. Yamada K, Goto S, Oyama T, Inoue N, Nagahiro S, Ushio Y. In vivo induction of the growth associated protein GAP43/B-50 in rat astrocytes following transient middle cerebral artery occlusion. Acta Neuropathol 1994; 88: 553–557.
66. Petito CK, Chung M, Halaby IA, Cooper AJ. Influence of the neuronal environment on the pattern of reactive astrocytosis following cerebral ischemia. Prog Brain Res 1992; 94: 381–387.
67. Eastwood SL, Harrison PJ. Synaptic pathology in the anterior cingulate cortex in schizophrenia and mood disorders. A review and a Western blot study of synaptophysin, GAP-43 and the complexins. Brain Res Bull 2001; 55: 569–578.
68. Hrdina P, Faludi G, Li Q et al. Growth-associated protein (GAP-43), its mRNA, and protein kinase C (PKC) isoenzymes in brain regions of depressed suicides. Mol Psychiatry 1998; 3: 411–418.
69. Benes FM, Lim B, Subburaju S. Site-specific regulation of cell cycle and DNA repair in post-mitotic GABA cells in schizophrenic versus bipolars. Proc Natl Acad Sci USA 2009; 106: 11731–11736.
70. Iwamoto K, Kakiuchi C, Bundo M, Ikeda K, Kato T. Molecular characterization of bipolar disorder by comparing gene expression profiles of postmortem brains of major mental disorders. Mol Psychiatry 2004; 9: 406–416.

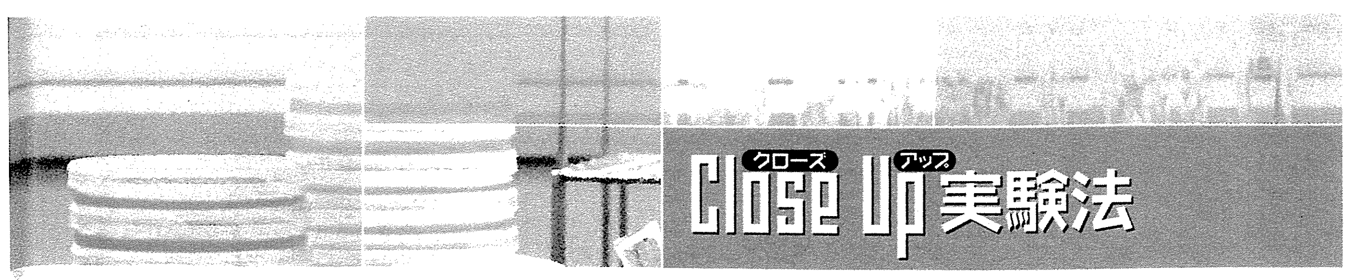

高感度に多型を検出するための エキソーム・シークエンシング

舟山　亮，長嶋剛史，中山啓子

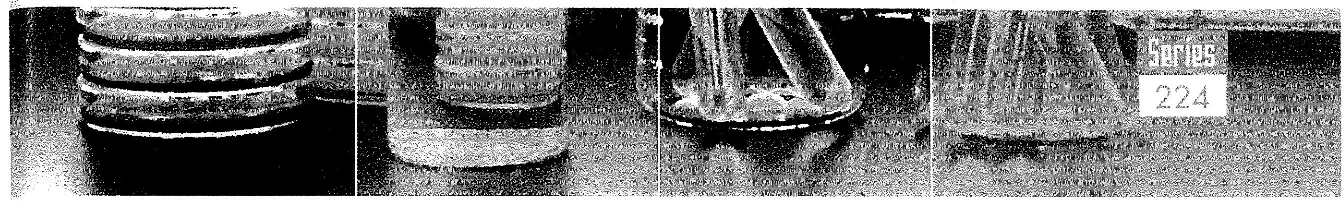

はじめに

ヒトゲノム30億塩基対のなかには，個人間で配列の異なる部位（多型）が約1千万カ所存在するといわれている．この遺伝的多様性は，個性を生み出す因子であると同時に，疾患を引き起こすリスク因子でもある．したがって，遺伝的多型の詳細なカタログを作成して，疾患との関連性を明らかにすることにより，遺伝的疾患の原因変異を正確に特定できるようになると期待されている．

次世代DNAシークエンシングは，解析できるDNA断片の数を革命的に増加させた，超ハイスループットな塩基配列決定法である．特に，疾患と直接的に関係するエキソン領域に的を絞ったエキソーム・シークエンシング（Exome-seq）は，全ゲノムを対象とした場合に比して低コストの遺伝子変異解析を可能にしている[1]．しかしながら，数千万塩基に及ぶエキソン領域のシークエンス解析では，すべての領域を偏りなく均等に解析するのは難しい．その結果，検出できない多型や偽陽性の多型が生じることがある．本稿では，サンプルの調製と塩基の読み取りの際に注意するべき点を中心に，高感度かつ高精度に多型を検出するためのExome-seq解析技術を紹介する．

原理

Exome-seqによる多型の検出法は，ゲノムDNAからエキソン領域を濃縮し，次世代シークエンサーにより配列を決定した後，参照ゲノムとの配列の違いを抽出する方法である（図1）．

まず，ゲノムDNAを断片化し，末端にアダプター配列を付加したライブラリを作製する．これをエキソン領域に相補的なビオチン標識プローブとハイブリッド形成させ，アビジンビーズを用いてエキソンを含むDNA断片を濃縮し，PCRで増幅する．ハイブリッド形成とPCR増幅は，多型の検出に大きく影響するステップである．ハイブリッド形成条件が不適切だと，エキソン濃縮率が低下し，多型の検出感度が低下する．PCRのサイクル数が多いと，重複リードの数が増加する（後述）．反応条件が最適化されたエキソン濃縮試薬が各社より販売されている．また，性能を比較した文献があるので，解析したい遺伝子領域や多型のタイ

Sensitive detection of genetic variants by Exome-sequencing
Ryo Funayama/Takeshi Nagashima/Keiko Nakayama : Division of Cell Proliferation, United Centers for Advanced Research and Translational Medicine, Tohoku University Graduate School of Medicine（東北大学大学院医学系研究科附属創生応用医学研究センター細胞増殖制御分野）E-mail : rfunayam@med.tohoku.ac.jp/nakayak2@med.tohoku.ac.jp

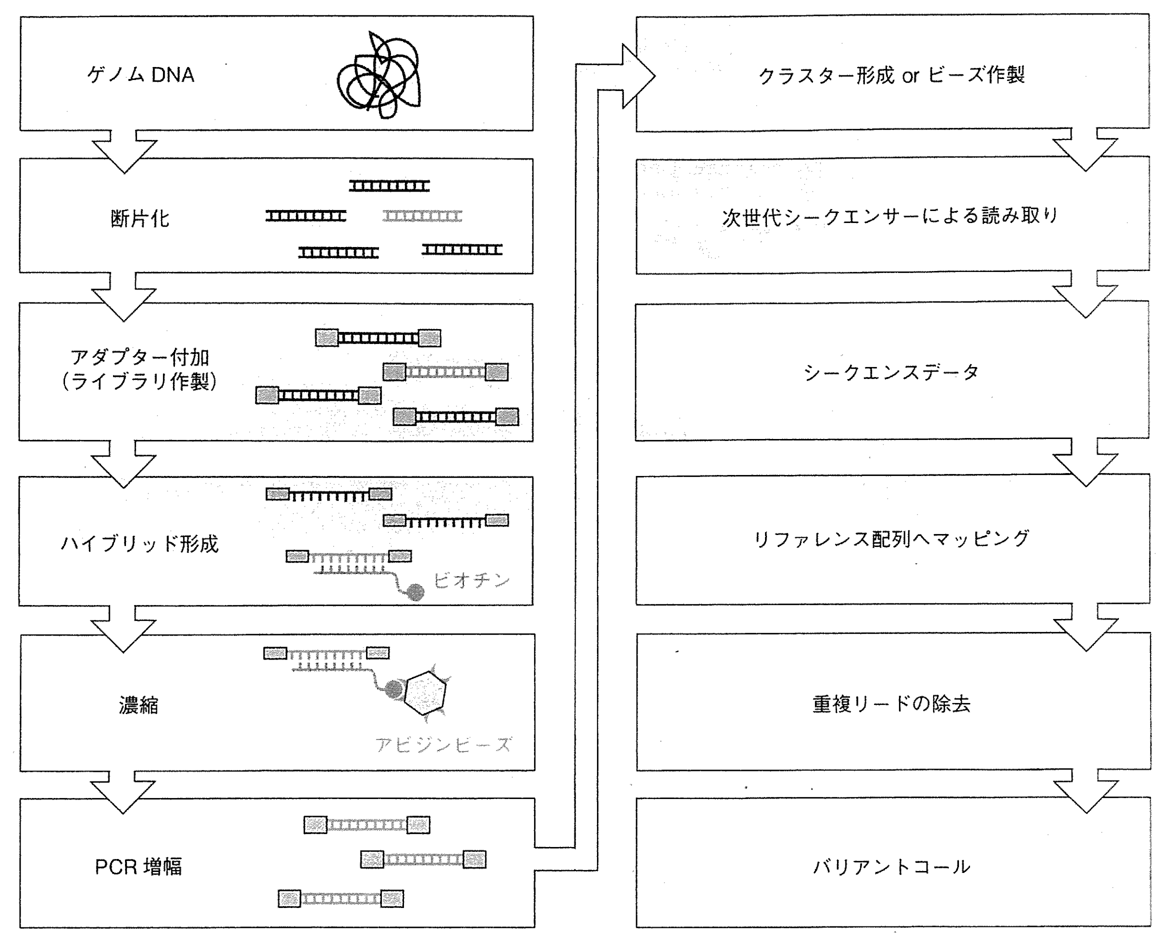

図1 Exome-seqによる多型の検出
解析は大きく分けて，ライブラリの作製とエキソン濃縮（▭），次世代シークエンサーによる配列解析（▭），および情報解析（▭）の3つのパートからなる

プを検討し，解析内容に適した試薬を選択するとよい[2)〜5)]．

情報解析では，読み取ったリードを染色体上にマッピングし，重複リード（duplicate read）を除いた後，参照ゲノムと異なる配列を多型として抽出する（バリアントコール）．重複リードとは，同一の染色体位置にマップされた複数のリードのことで，このうち1つだけをバリアントコールに使用するのが重複除去である．重複リードの除去は，特定のDNA断片がPCRにより濃縮されることによって，多型の検出精度が低下するのを防ぐために行う．重複除去されるリード数が多いと，バリアントコールに使用できるリード数が減り，結果として多型の検出感度が低下する．多型を高感度かつ高精度に検出するためには，重複リードの少ないライブラリを高いカバレッジで読み取ることが重要である．

以上の観点から，本稿では主に前半部分の「ライブラリ作製とエキソン濃縮」を最適化することにより検出精度を高めることに主眼をおいたプロトコールおよび注意点を紹介する．

準 備

- ゲノムDNA（20 ng/μL以上の濃度で1 μg）
- Quant-iT dsDNA BRアッセイキット（ライフテクノロジーズ社，Q32850）
- 超音波処理装置（Covaris社，S2）
- TruSeq DNA Sample Prepキット（イルミナ社，FC-121-1001）
- TruSeq Exome Enrichmentキット（イルミナ社，FC-121-1008）
- バイオアナライザ（アジレント・テクノロジーズ社，Agilent 2100）

プロトコール

1 ゲノムDNAの精製と定量

ゲノムDNAの精製は陰イオン交換カラムを用いた方法，またはフェノール・クロロホルム抽出法により行い，20 ng/μL以上の濃度で10 mM Tris-HCl（pH8.0）に懸濁する※1．酵素反応の条件を最適化するためには，DNAの正確な定量が重要である．吸光度を利用した核酸定量法はDNAとRNAを判別するのが難しいので，Quant-iT dsDNA BRアッセイキットのような蛍光色素を利用した定量法がよい．

2 ライブラリの作製とエキソン領域の濃縮

本稿では，解析対象領域が広く，遺伝子UTR（untranslated region）領域の解析能に優れた，イルミナ社のTruSeq Exome Enrichmentキットを用いた全エキソン濃縮方法を紹介する※2．

1. 超音波処理装置Covaris S2でゲノムDNA 1 μg（20 ng/μL）を断片化する※3．
2. TruSeq DNA Sample Prepキットを用いて，末端修復，3′-アデニル化，アダプターライゲーション，PCRの反応を行う※4．アダプターには6塩基のインデックス配列が含まれているので，複数のサンプルを処理する場合，各サンプルに異なるインデックスをもつアダプターを付加する．これにより，ステップ❹で最大6サンプルを混合して同時に処理することができる．PCRは10サイクルだけ行い，重複リードの増加を防ぐ．
3. バイオアナライザによる電気泳動を行い，ライブラリの断片長とDNA濃度を測定する（3で詳述）．
4. TruSeq Exome Enrichmentキットの推奨条件に従い，ライブラリDNA 500 ngとビオチン標識プローブとのハイブリダイ

※1 EDTAはライブラリ作製の酵素反応を阻害するので，使用する場合は0.1 mM以下にする．ゲノムDNAの品質はライブラリの収量に大きく影響する．

※2 イルミナ社のほかに，アジレント・テクノロジーズ社（SureSelect，G7544A #001），ロシュ・ダイアグノスティックス社（SeqCap EZ，6465684），ライフテクノロジーズ社（TargetSeq，A14060）がエキソン濃縮試薬を販売している．

※3 キットの推奨条件で処理する．200〜300 bpにピークをもつ，50〜1,000 bpの断片が得られる．ネブライザを用いて断片化してもよい．

※4 このキットは，酵素と反応バッファーがプレミックスされているため，反応液の調製が容易にできる反面，酵素活性が失われやすく，濃縮タイプの酵素と比べて消費期限が短いという欠点がある．キットを最初に使用する際，試薬を1回使い切りサイズに分注して保存し，消費期限内に使用するように注意する．

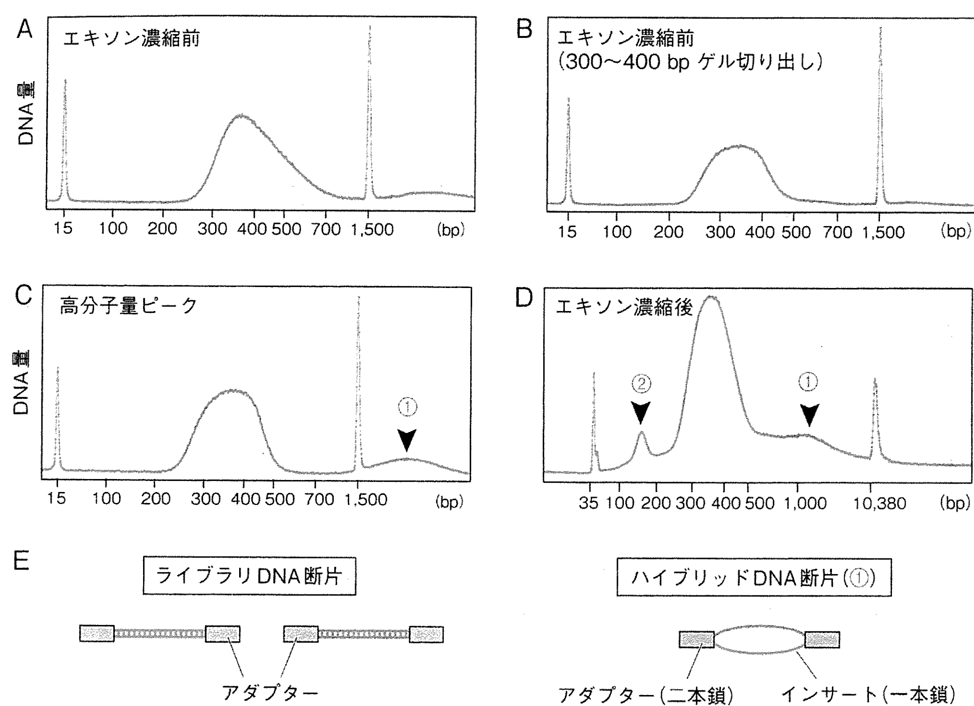

図2 ライブラリDNAの品質チェック
エキソン濃縮前のライブラリ（A〜C）をDNA 1000 chipで，濃縮後のライブラリ（D）をHigh Sensitivity chipで解析した．A）ゲル切り出しを行わずに作製したライブラリ．B）300〜400 bp領域を切り出して作製したライブラリ．C）高分子量DNA（①）を含むライブラリ．D）プローブ（②）が混入したエキソン濃縮後のライブラリ．E）相補的なインサート配列をもつDNA断片（左）とアダプター領域でのみ塩基対形成したハイブリッドDNA断片（右）

ゼーションを行う※5．

❺濃縮後のライブラリをバイオアナライザで解析する．また，リアルタイムPCRによりDNAを定量する（❸で詳述）．

❸ ライブラリDNAの品質チェック

エキソン濃縮前後のライブラリをバイオアナライザにより解析し，DNA断片長を評価する※6．濃縮前のライブラリは400 bp付近にピークをもつ，250〜1,000 bpの断片長となる（図2A）．アダプターライゲーション後のステップでアガロースゲル電気泳動を行い，300〜400 bpのDNAをサイズセレクトすると，より均一な断片長のライブラリを作製できる（図2B）．しかし，サイズセレクトは通常必要でない．

ライブラリのなかには，高分子量のDNAピークをもつものがしばしばある（図2C，D①）．これは，異なるインサート配列をもつ一本鎖のDNA断片が，アダプター部分で塩基対形成した分子ではないか，とわれわれは考えている（図2E）．エキソン濃縮後のライブラリには，ビオチン標識プローブが混入することがある（図2D②）※7．

次に，ライブラリDNA濃度を測定し，収量を評価する．濃縮前の

※5 反応中にチューブのフタが開かないように注意する．

※6 濃縮前のライブラリはDNA 1000 chipで，濃縮後のライブラリはHigh Sensitivity chipで解析するとよい．

※7 高分子量のDNAやビオチン標識プローブは，多少混入しても，その後の解析には影響しないようである．

定量はバイオアナライザで行ってもよい．ただし，サンプル間で読み取るリード数を均一にしたい場合，リアルタイムPCRで正確に定量してから，サンプルを混合するとよい．特に，高分子量ピークがみられたサンプルは，バイオアナライザでは正確に定量できない．濃縮後のライブラリは，リアルタイムPCRで定量する．通常，1 μgのゲノムDNAから，500～900 ngのライブラリ（濃縮前）が得られる※8．500 ngのライブラリをエキソン濃縮すると，最終的に20～60 nMのライブラリ30 μLが得られる．

4 クラスター形成と次世代シークエンス解析

作製したライブラリから少量を分取して1 nMに希釈し，クラスターを形成させる※9．次世代シークエンサーによる読み取りは，70～100塩基ずつのペアエンドで行う．読み取った塩基配列から多型を抽出する情報解析の方法については，文献6などを参照されたい．

※8 サンプルや試薬が劣化すると，収量が大きく低下することがある．収量を上げるためにPCRサイクル数を増やすと，重複リードが増加するので気をつける．

※9 Bridge PCR反応により基盤（フローセル）上で増幅した1分子由来のDNAの集まりをクラスターという．クラスターの密度を最適にするために，ライブラリの定量を正確に行う．

実験例

本法を用いてヒトゲノムの多型を検出した実験結果の例を図3に示す．末梢血由来ゲノムDNA 1 μgからライブラリを作製し，エキソン領域を濃縮後，イルミナ社のGenome Analyzer IIxを用いて，ペアエンドで70塩基ずつシークエンス解析した．読み取ったリードのなかから，シングルエンド9,000万リード，ペアエンド4,500万ペアリード（計9,000万リード）をそれぞれ無作為に抽出した．重複リードを除いた後，バリアントコールを行い，読み取り方式が多型の検出感度に与える影響を比較した．

マップ率はほぼ100％で，読み取り方式による違いはみられなかったが，ペアエンド読み取りでは重複除去されたリード数が少なかった（図3A）．ペアエンドでは，「重複」の判定基準を厳しく設定することが可能なので，除去されるリード数を少なくできるためである．その結果，ペアエンド読み取りではバリアントコールに使用できるリード数がシングルリード読み取りより多く，結果として検出できた多型の数が多かった（図3B）．

われわれの経験では，TruSeq Exome Enrichmentキットを用いて作製したライブラリを1億リード読み

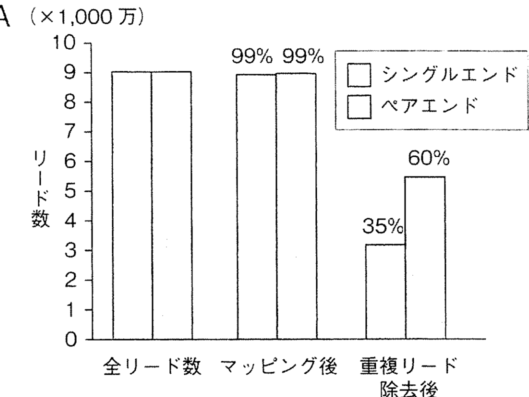

B

	検出された多型の数	
	シングルエンド	ペアエンド
合計	57,302	79,376
SNV	50,533	66,715
Indel	6,769	12,661
既知	53,949	72,160
新規	3,353	7,216

図3 多型の検出例
A）解析ステップごとのリード数の推移．パーセントは全リード数に対する割合を示す．B）検出された多型の数．dbSNPまたは1000 Genomesのいずれかに登録されているものを既知，どちらにも登録されていないものを新規とした．SNV：single nucleotide variant，Indel：insertion and deletion

取った場合，重複除去されるリードの割合は10～40％である．しかし実験によっては，約80％が重複除去されてしまい，カバレッジが低下してしまったことがある．原因は不明だが，ハイブリッド形成またはPCR反応に何らかの問題があったと考えている．

おわりに

多型を高感度に検出するためには，重複リードの少ないライブラリを長く読み取ることにより，カバレッジを高めることが重要である．初発DNAの品質低下，PCRサイクル数の過度の増加や不適切なハイブリダイゼーション条件は，重複リードを生み出す原因となるので注意が必要である．Exome-seqは，全ゲノム・シークエンシングに比べるとコスト効率の高い解析手法であるが，1家系（5～6検体）を解析するのに100～200万円の試薬代が必要な現状を考えると安価な手法とは言いがたい．今後，各工程の条件をさらに最適化することで限られたリード数を有効に利用して，高感度に多型を検出できるように工夫したい．

文献

1）Teer, J. K. & Mullikin, J. C.：Hum. Mol. Genet., 19：R145-151, 2010
2）Clark, M. J. et al.：Nat. Biotechnol., 29：908-914, 2011
3）Sulonen, A. M. et al.：Genome Biol., 12：R94, 2011
4）Asan et al.：Genome Biol., 12：R95, 2011
5）Parla, J. S. et al.：Genome Biol., 12：R97, 2011
6）DePristo, M. A. et al.：Nat. Genet., 43：491-498, 2011

● 筆頭著者プロフィール ●

舟山　亮：2007年，東京工業大学大学院生命理工学研究科博士後期課程修了．理学博士．京都大学大学院生命科学研究科博士研究員，同科特任助教を経て，'07年10月より現所属（助教）．次世代シークエンサーを利用した解析のサポートをしながら，がん細胞のエピゲノムと遺伝子発現制御機構に興味をもって研究している．

Book Information

よくわかる ゲノム医学 大好評！

ヒトゲノムの基本からテーラーメード医療まで

監修／菅野純夫　著／服部成介，水島-菅野純子

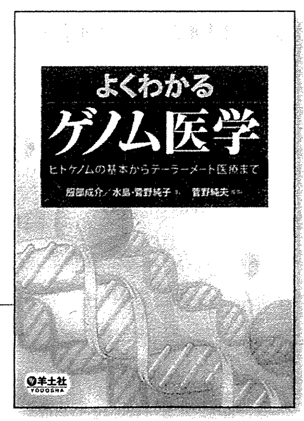

ゲノム医学のエッセンスを体系的に解説．個人個人のゲノムに合わせた創薬・治療が当たり前になりつつある時代．知っておくべき知識が豊富なイラストとわかりやすい文章でしっかり身につく！

◆定価（本体 3,500円＋税）
◆2色刷り　B5判　206頁
◆ISBN978-4-7581-0928-4

ゲノム情報の医療への応用がわかりやすく学べる最適な教科書

発行 羊土社

ARTにおけるエピジェネティクス異常

有馬隆博* 樋浦 仁* 岡江寛明* 佐藤晶子* 宮内尚子* 阿部千鶴* 林 千賀*

近年，晩婚化の社会情勢と医療技術の進歩により，ARTは一般に普及している。しかし，同時にこれまで非常に稀であったインプリンティング異常症の発症頻度が増加していることが世界中で報告され，注目されている。ARTは，インプリンティングが獲得される時期の配偶子を操作するため，排卵誘発，配偶子操作，培養液などのメチル化（エピジェネティクス）への影響について懸念されている。早急に異常を起こすリスク要因の検索と今後の追跡調査について十分な検討を行わなければならない。

はじめに

『エピジェネティクス』とは，DNAの配列に変化を起こさず，かつ細胞分裂を経て伝達される遺伝子機能の変化やその仕組みで，ゲノムの遺伝情報を正しく発現し，細胞の状態を正確に記憶する生命システムである。具体的には，DNAメチル化，ヒストン修飾，クロマチン構造などを介する遺伝子発現制御が主体であり，発生・分化・リプログラミングに関与する。その代表例として挙げられるゲノムインプリンティング（遺伝子刷り込み）やX染色体の不活化は，マウスをはじめヒト疾患の解析により，配偶子形成過程（卵子，精子の形成）や初期発生胚に極めて重要であることが判明してきた。

近年，晩婚化，少子化の社会情勢に加え，医療技術の進歩によりARTは普及し，多くの出生児を誕生させている。しかし，ART出生児に，これまで非常に稀であったインプリンティング異常症の発生頻度の増加も指摘されている。ARTは，インプリンティングが獲得される時期の配偶子を操作するため，排卵誘発，配偶子操作，培養液などのメチル化異常への影響について懸念されている。しかしながら，ARTを受ける患者が一般の人口統計と異なる特殊な集団であるため，単純にART治療がそのような危険を引き起こすのか，正確に評価することは難しい。ART治療を受ける患者は，一般に低い妊娠率で，比較的高齢である。そのため胎児，新生児異常と関連することも考えられる。本稿では，不妊症男性のうち特に乏精子症患者精子に高頻度にみられるインプリンティング異常の存在と，全国規模のインプリンティング異常症とARTとの関連についてその実態について紹介する。

* Takahiro Arima, Hitosi Hiura, Hiroaki Okae, Akiko Satou, Naoko Miyauchi, Chizuru Abe, Chika Hayashi 東北大学大学院医学系研究科環境遺伝医学総合研究センター情報遺伝学分野